Annu. Rev. Mater. Res. 2018.48:219-243. Downloaded from www.annualreviews.org
Access provided by Copenhagen University on 05/07/22. For personal use only.

ANNUAL REVIEWS

Annual Review of Materials Research

High-Temperature Dielectric Materials for Electrical Energy Storage

Qi Li,[1] Fang-Zhou Yao,[2,3] Yang Liu,[2] Guangzu Zhang,[2] Hong Wang,[3,4] and Qing Wang[2]

[1]State Key Laboratory of Control and Simulation of Power System and Generation Equipments, Department of Electrical Engineering, Tsinghua University, Beijing, 100084, China

[2]Department of Materials Science and Engineering, The Pennsylvania State University, University Park, Pennsylvania 16802, USA; email: wang@matse.psu.edu

[3]State Key Laboratory for Mechanical Behavior of Materials, Xi'an Jiaotong University, Xi'an, 710049, China

[4]Department of Materials Science and Engineering, Southern University of Science and Technology, Shenzhen, 518055, China; email: wangh6@sustc.edu.cn

Annu. Rev. Mater. Res. 2018. 48:219–43

First published as a Review in Advance on February 28, 2018

The *Annual Review of Materials Research* is online at matsci.annualreviews.org

https://doi.org/10.1146/annurev-matsci-070317-124435

Copyright © 2018 by Annual Reviews.
All rights reserved

ANNUAL REVIEWS **Further**

Click here to view this article's online features:

- Download figures as PPT slides
- Navigate linked references
- Download citations
- Explore related articles
- Search keywords

Keywords

dielectric polymers, electroactive ceramics, high temperature, energy storage, capacitors

Abstract

The demand for high-temperature dielectric materials arises from numerous emerging applications such as electric vehicles, wind generators, solar converters, aerospace power conditioning, and downhole oil and gas explorations, in which the power systems and electronic devices have to operate at elevated temperatures. This article presents an overview of recent progress in the field of nanostructured dielectric materials targeted for high-temperature capacitive energy storage applications. Polymers, polymer nanocomposites, and bulk ceramics and thin films are the focus of the materials reviewed. Both commercial products and the latest research results are covered. While general design considerations are briefly discussed, emphasis is placed on material specifications oriented toward the intended high-temperature applications, such as dielectric properties, temperature stability, energy density, and charge-discharge efficiency. The advantages and shortcomings of the existing dielectric materials are identified. Challenges along with future research opportunities are highlighted at the end of this review.

Annu. Rev. Mater. Res. 2018.48:219-243. Downloaded from www.annualreviews.org
Access provided by Copenhagen University on 05/07/22. For personal use only.

1. INTRODUCTION

Dielectric materials form the basis of one of the most fundamental passive components known as dielectric capacitors, which are present in almost every sort of electronic circuit (1–6). The function of dielectric capacitors is to store electric energy by holding opposite charges on electrodes separated by an insulator, the dielectric material. Dielectric capacitors are special among the various electrical energy storage devices, e.g., batteries, because they can release the stored energy in an extremely short period of time (on a microsecond scale) to create intense power pulses (7–10). This capacity enables many pulsed power applications such as medical defibrillators, transversely excited atmospheric lasers, and advanced electromagnetic systems, in which capacitors convert a low-power, long-time input into a high-power, short-time output. Lately, emerging products related to renewable energy, such as hybrid electric vehicles (HEVs), grid-tied photovoltaics, and wind turbine generators, have created a great demand for dielectric capacitors, as they are vital electronic elements for the conversion of collected/stored direct current (dc) to alternating current (ac) energy (11, 12).

The urgent need for the high-temperature capability of dielectric capacitors comes from the recent boom in, among many other areas (13), the avionic and automotive industries (14, 15), underground oil and gas explorations (16), and advanced propulsion systems (17), in which high power, high current, and elevated-temperature conditions are present (**Figure 1**). In HEVs, the

Figure 1

Emerging applications demanding high-temperature dielectric capacitors, including hybrid electric vehicles, wind turbine generators, avionic industries, underground oil and gas explorations, and advanced propulsion systems.

underhood temperature can be more than 140°C. Power inverters represent one of the most important electronic components of HEVs and are used to convert dc electricity supplied by batteries to the ac power needed to drive the traction motor. Capacitors constitute the major component of power inverters; e.g., in Toyota Prius® HEVs, capacitors account for ∼40% of the cost and ∼35 vol% and ∼23 wt% of the inverter. The mainstream capacitors currently employed in power inverters use biaxially oriented polypropylenes (BOPP) as the dielectric. The mismatch between ambient temperature (140°C) and the maximum operating temperature of BOPP [∼105°C (18)] requires either active cooling systems to be involved or all the electronic devices and circuitries to be redesigned and remanufactured. The present strategy of manufacturers is to introduce a secondary cooling system set at ∼65°C in addition to the engine radiator for stable operation of power inverters (19). This auxiliary cooling loop brings in extra weight, volume, and complexity in the design of power systems, and such factors are unfavorable for both the manufacturing cost and performance of HEVs (20–23).

In other applications, the local temperature of electronic devices is also higher than the maximum operating temperature of BOPP, while creation of the physical space could be costly or even impossible. One example is the development of a more electric aircraft (15). The need for high-temperature dielectric materials (up to 250°C) arises from the proximity of the power electronics to the heat sources involving turbine engines, generators, and motors, as well as control and sensing electronics placed near the outer shells of rockets and space shuttles (13, 16). Under some circumstances, cooling may not be practical. In underground oil and gas explorations, temperatures can exceed 200°C, and heating is not confined locally to electronics in the drill (16). Under such harsh environmental conditions, cooling is ineffective, and electronic systems have to operate at high temperatures.

To meet these demanding requirements, there has been considerable research interest in high-temperature capabilities of dielectric materials (13, 24, 25). Yet major challenges and limitations exist. This review provides an overview of the currently available high-temperature dielectric materials (>150°C rated), describing their advantages and potential, together with some of the fundamental and technical issues to be addressed. We conclude by highlighting some challenges and opportunities for future developments. In particular, focus is on dielectric polymers, polymer nanocomposites, and ceramics, as they are currently the most important and promising classes of dielectric materials in the areas of high-temperature power systems and electronic component technologies.

2. GENERAL CONSIDERATIONS FOR HIGH-TEMPERATURE DIELECTRIC MATERIALS

There have been many review articles on advancing capacitor dielectrics (26–31), but these articles focus mainly on room temperature applications. The design of high-temperature dielectric materials, however, is different and should therefore be reconsidered to fulfill a stringent set of requirements in high-temperature capacitor applications.

2.1. Thermal Stability

Thermal stability is a prerequisite for reliable insulating properties under high-temperature conditions because this quality determines the ability of materials to resist collapse of physical integrity under thermal stress. In the temperature span covering most of the intended applications (i.e., room temperature to 350°C), ceramics are the most thermally stable, and dielectric polymers are, by contrast, very susceptible to thermal stress. For most dielectric polymers, the glass transition

Annu. Rev. Mater. Res. 2018.48:219-243. Downloaded from www.annualreviews.org
Access provided by Copenhagen University on 05/07/22. For personal use only.

temperature (T_g) is less than 100°C (32). Amorphous polymers lose their stiffness and exhibit an abrupt change in physical properties as temperature increases to above T_g. For instance, thermal excursions through T_g dramatically increase the free volume in a polymer material, i.e., the space not occupied by polymer molecules, and hence lead to significantly fluctuating dielectric properties. In addition, a high free volume and high mobility of polymer chains would allow for considerable electronic and ionic conduction due to the ease of propagation of charge carriers across the material. These issues are closely related to the stability, reliability, and service lifetime of polymer dielectrics at elevated temperatures, and therefore T_g is usually the basic criterion in the assessment of high-temperature polymer dielectric materials. For polymers with very high crystallinities, where the crystalline phase plays a dominant role, the melting point (T_m) is also used to evaluate temperature capability.

As both T_g and T_m are controlled mainly by main-chain stiffness, they are usually coupled in homopolymers. To obtain higher values of T_g and T_m, a very common method is to incorporate rigid structural units into the main chains of polymers to impede rotation and improve stiffness of the main chains. Alternatively, the presence of bulky side groups is also very effective in securing high T_g and T_m values, as such side groups physically restrict bond rotation. Moreover, when the side groups are polar, they restrict the rotation further as a result of polar interactions. A third approach is to create intermolecular chemical cross-links that strongly restrict molecular motion. For some highly cross-linked polymers, the glass transition may not even occur (32).

2.2. Dielectric Breakdown Models

Dielectric breakdown strength (E_b) is the electric field at which a rapid reduction in the resistance of an electrical insulator is observed when that field is applied on the dielectric material. E_b is one of the governing parameters for the energy storage density of capacitors; e.g., the energy density of a linear dielectric material scales with the square of electric field according to

$$U = 0.5\varepsilon_0\varepsilon_r E^2, \quad 1.$$

where U is the energy density, ε_0 is the permittivity of vacuum, ε_r is the relative permittivity, and E is the electric field. Among the many breakdown mechanisms of polymer dielectrics, free volume breakdown, electromechanical breakdown, and thermal breakdown have the greatest chance of occurring under high-temperature conditions (33–35) and thus need particular consideration.

Free volume breakdown is a process in which electrons are accelerated in the free volume of polymers to energies sufficient to create free electron–hole pairs via collisions with bound electrons and to eventually cause the failure of dielectrics (33). Polymer materials have a large increase in free volume approximately at T_g, again necessitating high T_g of polymer dielectrics for high-temperature applications. Cross-linking is commonly accepted as an efficient route to reduce and restrict the free volume and is therefore favorable for improving the breakdown strength of polymer dielectrics (8, 36).

The electromechanical breakdown model concerns the mechanical collapse associated with the Maxwell stress exerted by the applied electric field (34). This type of breakdown is usually observed in soft polymer dielectrics such as polyethylene because the critical field E_b is dependent on the mechanical strength of the material, given by

$$E_b = 0.606\left(\frac{Y}{\varepsilon_0\varepsilon_r}\right)^{0.5}, \quad 2.$$

where Y is the Young's modulus, ε_0 is the permittivity of vacuum, and ε_r is the relative permittivity. Since the elastic modulus of a polymer material usually decreases with rising temperature, and

Annu. Rev. Mater. Res. 2018.48:219-243. Downloaded from www.annualreviews.org
Access provided by Copenhagen University on 05/07/22. For personal use only.

especially when the temperature increases beyond T_g or T_m, this specific breakdown mechanism becomes applicable to many polymers in the high-temperature region.

Thermal breakdown describes the catastrophic thermal runaway of dielectric materials as the rate of heat generation within the material due to dissipation in an applied electric field exceeds the rate of heat loss to the external medium (35). This exceedingly complicated and nonlinear process, which is poorly understood at the microscopic level, can be expressed macroscopically as

$$\rho_m C \frac{\partial T(\mathbf{x})}{\partial t} = K\nabla^2 T(\mathbf{x}) + \sigma(\mathbf{x}, T)E^2. \quad 3.$$

Here ρ_m and C are the density and heat capacity, respectively; σ is the electrical conductivity; K is the thermal conductivity; and E denotes the applied electrical field (37). At elevated temperatures, the conduction loss of polymer dielectrics becomes much more significant compared with that at room temperature owing to the many temperature-dependent conduction mechanisms (some of which are discussed in Section 2.3), which leads to the production of a vast amount of Joule heat.

As polymer materials have relatively low thermal conductivities, i.e., within the range of 0.2–0.5 W/(m·K), heat cannot be conducted away fast enough and so accumulates, causing the temperature to rise eventually. Under continuous operation, the device may fail due to thermal breakdown of dielectric materials. The underlying mechanism of thermal breakdown implies that a high value of T_g or T_m is not adequate to protect polymer dielectrics against this type of failure under high-temperature conditions, because heat conduction occurs at a much lower rate than does heat generation. Under continuous operation of capacitors without an active cooling system, the internal temperature of a device can exceed the rated value provided by the present level of thermal stability of polymer materials. More reasonable ways to tackle this issue are (*a*) suppression of conduction losses to mitigate the internal heating and (*b*) improvements in the efficiency of heat transfer to keep the material relatively cool.

The breakdown strength of inorganic dielectrics is closely associated with the intrinsic bandgap of the materials and can be significantly influenced by extrinsic factors, such as defect chemistry, sample thickness, grain size, and structural configuration. A thermochemical model describes the fundamental relationship between dielectric breakdown strength and dielectric constant, where breakdown strength is approximately inversely proportional to the square root of the dielectric constant (38). The high local electric fields in high-dielectric-constant materials may make the polar molecular bonds vulnerable by standard Boltzmann processes and/or by hole capture. Consequently, the vulnerability of the polar molecular bonds lowers breakdown strength.

2.3. Conduction Mechanisms

Under high electric fields and elevated temperatures, significant leakage current occurs in many polymer dielectrics due to emerging conduction events (39–42), including those occurring in the material bulk and at the electrode-dielectric interface. Leakage current can lead to continuous energy loss and undesirable temperature rise inside the dielectrics. This energy loss–induced temperature rise is highly detrimental in the context of high-temperature capacitor applications, given that thermal runaway is one of the main factors limiting the temperature ratings and voltage ratings of film capacitors.

Almost all conduction mechanisms in polymers—such as ohmic conduction, ionic conduction, hopping conduction, Poole-Frenkel emission, Schottky emission, and thermionic-field emission—increase with temperature, usually exponentially (39, 41). Poole-Frenkel emission and Schottky emission are among the most often seen conduction mechanisms in the high-temperature region.

Annu. Rev. Mater. Res. 2018.48:219-243. Downloaded from www.annualreviews.org
Access provided by Copenhagen University on 05/07/22. For personal use only.

Poole-Frenkel emission belongs to the bulk-limited type of conduction mechanisms related to the trap energy level in polymer dielectrics. When charge carriers constrained in a trapping center obtain enough energy to overcome the potential barrier, they are excited to the conduction band, and electric current is observed. In particular, if the energy is from thermal excitation, the conduction falls within the category of Poole-Frenkel emission. Schottky emission, sometimes referred to as thermionic emission, denotes a phenomenon in which charge carriers in a metal electrode can overcome the energy barrier at the metal-dielectric interface to be injected into the dielectric when they obtain enough energy from thermal activation. Schottky emission is an electrode-limited conduction mechanism, as it is governed by the barrier height at the metal-dielectric interface.

The above conduction models predict that electric conduction in polymer dielectrics is much more significant at elevated temperatures than at room temperature, suggesting that the rising temperature dramatically increases the probability of thermal runaway. The environmental temperature can have an even greater impact under high electric fields due to field-dependent conduction mechanisms; i.e., the leakage current increases exponentially with increasing electric fields beyond the critical point at which conduction is no longer ohmic (39, 41, 42). Similar to the scenario in polymer dielectrics, the above conduction mechanisms are applicable to inorganic dielectric films as well. However, for inorganic bulk dielectrics, ohmic conduction is valid at low applied fields, and space charge–limited conduction dominates close to the breakdown field (43).

2.4. Relative Permittivity and Dissipation Factor

The relative permittivity (ε_r, also commonly known as dielectric constant) of a dielectric material is the ratio of (*a*) the capacitance of a capacitor adopting that dielectric to (*b*) the capacitance of a similar capacitor using vacuum as its dielectric. As Equation 1 shows, the energy storage density of a dielectric material is directly proportional to ε_r, which implies that the specific energy density of a dielectric capacitor can be improved by using a dielectric material with high ε_r values or that, in turn, the physical size of the capacitor can be reduced to meet a given energy specification. The miniaturized capacitors would help to reduce space and weight in HEVs and aerospace applications. It would reduce the overall cost of printed circuit boards, which is typically calculated on the basis of area. With inadequate energy densities, dielectric capacitors have to operate at a high repetition rate of charge-discharge cycles, which may cause deleterious effects such as accelerated heating and fast aging (10, 19).

Dissipation factor, or dielectric loss tangent, is a measure of the rate of energy loss during polarization and depolarization of dielectric materials. It occurs when the relaxation time and the frequency of the applied field are similar. This form of energy loss not only deteriorates energy storage capability but also builds up equivalent series resistance (ESR) coupled with the capacitor (19). In high-current circuitries, ESR is harmful, as it contributes to continuous heating. It is therefore desirable to maximize ε_r while maintaining a low dissipation factor of dielectrics in capacitor applications. Since the polarization and relaxation of electrical charges and dipoles are dependent on both temperature and time, ε_r values (and hence the capacitance) and dissipation factor are usually variable with respect to temperature and electric field frequency. The relevant standard of Electronic Industries Alliance (Arlington, VA) defines commercial X7R capacitors as having less than $\pm 15\%$ deviation of capacitance from the room temperature value over the temperature range of -55 to 125°C, while ceramic chip-on-glass capacitors possess temperature coefficients of capacitance of 0 ± 30 ppm/°C. This standard provides the guideline for some high-temperature dielectrics.

Annu. Rev. Mater. Res. 2018.48:219-243. Downloaded from www.annualreviews.org
Access provided by Copenhagen University on 05/07/22. For personal use only.

Table 1 Overview of high-temperature polymer dielectric films from commercial sources

Trade name (dielectric)	T_g (°C)	ε_r (at 1 kHz)	Dissipation factor (at 1 kHz) (%)	Dielectric strength (MV/m) (film thickness in parentheses)	Volume resistivity (Ω · cm)
Kapton (PI)	360–410	2.7–3.5	0.13–0.26	154–303 (7.6–127 μm)	2.3×10^{17}
UPILEX (PI)	285–500	3.2–3.5	0.13–0.7	147–320 (12.5–125 μm)	10^{16}–10^{17}
ULTEM (PEI)	217–247	3.15	0.12	200 (25 μm)	1.0×10^{17}
ISARYL (FPE)	330	3.2–3.5	0.31–0.7	220–320 (100–120 μm)	10^{15}–10^{17}
Cyclotene (BCB)	>350	2.75	0.12	300 (10 μm)	1.0×10^{18}
TORELINA (PPS)	118	3.0	<0.1	490 (9 μm)	1.0×10^{16}
KetaSpire (PEEK)	150	3.1	0.3	150 (50 μm)	2.6×10^{16}
Kepstan (PEKK)	162	2.6	0.7	84 (100 μm)	1.0×10^{16}

Abbreviations: BCB, divinyltetramethyldisiloxane-bis(benzocyclobutene); FPE, fluorene polyester; PEEK, poly(ether ether ketone); PEI, poly(ether imide); PEKK, poly(ether ketone ketone); PI, polyimide; PPS, poly(phenylene sulfide).

Annu. Rev. Mater. Res. 2018.48:219-243. Downloaded from www.annualreviews.org
Access provided by Copenhagen University on 05/07/22. For personal use only.

3. HIGH-TEMPERATURE DIELECTRIC MATERIALS

3.1. High-T_g Polymers

The advantages of polymer dielectrics for capacitor applications have been well documented and include high breakdown strength, low mass density, inexpensive production, flexibility, and ease of processing (4, 7, 18). In this section, the promise of state-of-the-art high-temperature polymer dielectric films from both commercial sources (with basic information compiled in **Table 1** and chemical structures summarized in **Figure 2**) and noncommercial sources for capacitor applications are discussed, and relevant studies concerning structural modifications of these polymers are reviewed.

3.1.1. Polyimide and poly(ether imide). Polyimide (PI) is a thermoset polymer synthesized from dianhydride and diamine (or diisocyanate) monomers through a condensation reaction followed by chemical imidization (44, 45). PIs are characterized by exceptional resistance to heat and chemicals and decent mechanical strength; these characteristics stem from the imide structure in the main chain (46), which, in conjunction with the aromatic structure, results in very high T_g values up to 500°C. PIs also have excellent insulating properties, including low dissipation factor, high breakdown strength, and high volume resistivity, in addition to an ε_r that is 50% higher than that of polypropylene (PP). The good thermal stability and outstanding dielectric performance make PIs a good candidate for high-temperature film capacitor applications.

Kapton® is a typical example of a PI and was developed by DuPont in the late 1960s. The low dissipation factor and high breakdown strength of Kapton are well retained up to 200°C (24, 36, 47). But under high electric fields, the high-temperature dielectric performance is much inferior to that at room temperature (37). For instance, under an electric field of 200 MV/m and at 150°C, the conduction loss of Kapton is as high as 24%; i.e., 24% of stored energy is dissipated in the form of Joule heat, resulting in a 76% charge-discharge efficiency (η) and a relatively low dischargeable energy density of ~0.44 J/cm^3 (**Figure 3**). With further increases in temperature, the conduction loss is even larger. At 250°C, the conduction loss of Kapton is almost 100%, suggesting that the upper bound of the high-field operating temperature of Kapton is much below

Annu. Rev. Mater. Res. 2018.48:219-243. Downloaded from www.annualreviews.org
Access provided by Copenhagen University on 05/07/22. For personal use only.

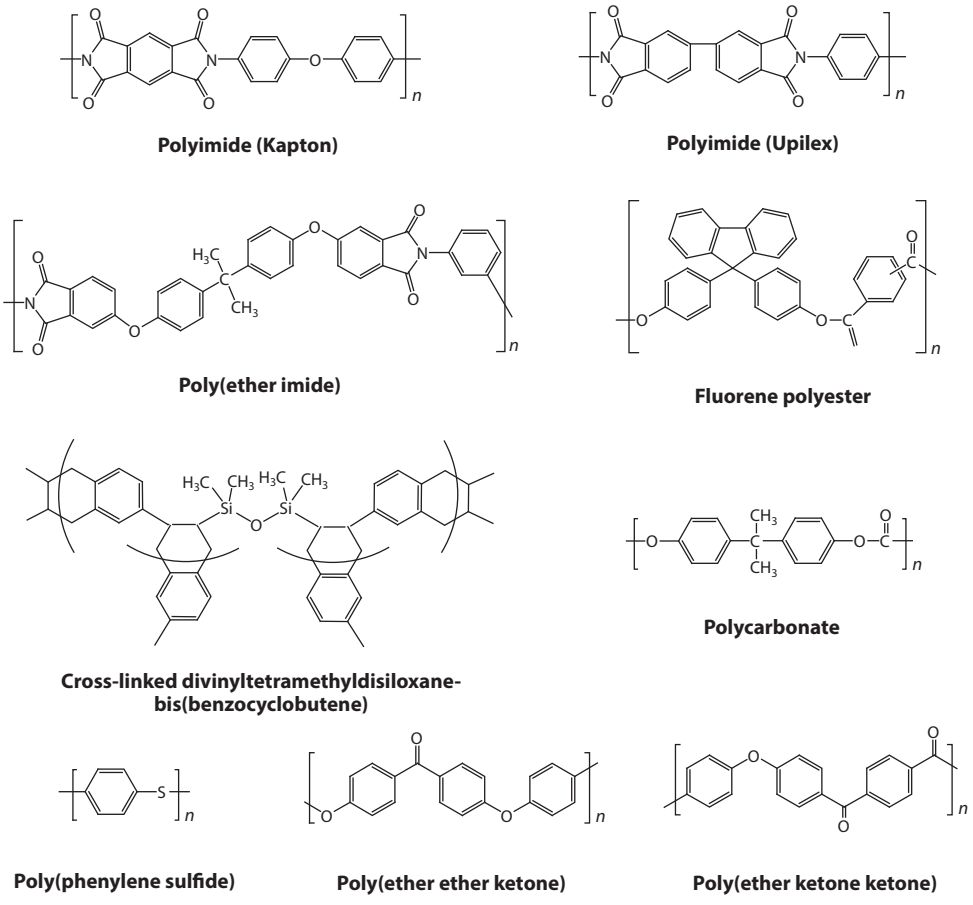

Figure 2

Chemical structures of various high-temperature polymer dielectrics.

its T_g value. It is argued that the presence of a diphenylether moiety in Kapton has an adverse effect on the thermal-oxidative resistance (48). In addition, the imide ring structure in the main chain endows PIs with unfavorable moisture sensitivity and high water uptake. For film capacitor applications, these issues can be addressed by impregnating the windings with an insulating fluid and by hermetically sealing the interior.

Poly(ether imides) (PEIs), a modified version of PI, are amorphous dielectric polymers with improved processability at the expense of compromised thermal stability with respect to PIs. The improved processability and reduced thermal stability are due to the presence of flexible ether linkages incorporated into the backbone of PEIs through the nucleophilic aromatic substitution of leaving groups from phthalic anhydride by bisphenol A. The most important commercial PEI product is ULTEM® by SABIC, with T_g ranging from 217°C to 247°C. The ε_r and the dissipation factor of PEIs are similar to those of PIs. Unexpectedly, the energy storage properties of PEIs are better than those of PIs up to 200°C. For example, the dischargeable energy density and η of PEIs are 0.5 J/cm^3 and 90%, respectively, under an electric field of 200 MV/m and at 150°C (36) (**Figure 3**). Even at 200°C, a temperature very close to the T_g value, the η of PEIs still approaches

Annu. Rev. Mater. Res. 2018.48:219-243. Downloaded from www.annualreviews.org
Access provided by Copenhagen University on 05/07/22. For personal use only.

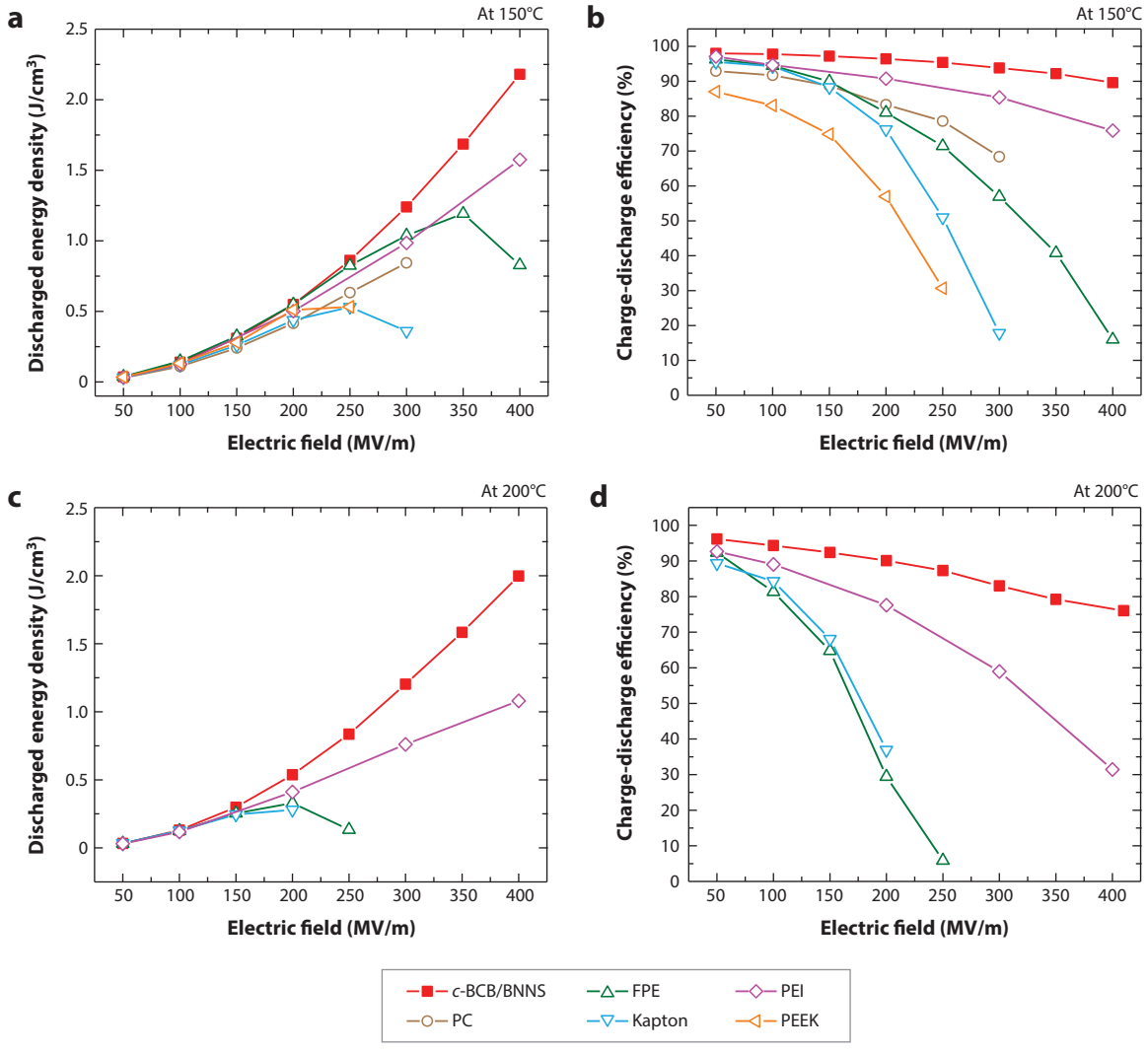

Figure 3

(*a*,*c*) Electric field–dependent discharged energy density and (*b*,*d*) charge-discharge efficiency of high-temperature polymer-based dielectrics measured at 150°C and 200°C. Abbreviations: *c*-BCB/BNNS, cross-linked divinyltetramethyldisiloxane-bis(benzocyclobutene)/boron nitride nanosheet; FPE, fluorene polyester; PC, polycarbonate; PEEK, poly(ether ether ketone); PEI, poly(ether imide). Adapted with permission from Reference 37. Copyright © 2015, Nature Publishing Group.

80%. Chemically modified PEIs have a greater ε_r; e.g., cyano-PEIs are reported to offer an ε_r of ~4.6 (49).

One of the major drawbacks of PIs with regard to high-temperature film capacitor applications may arise from the high temperature coefficient of ε_r [also known as the temperature coefficient of capacitance (TCC)]. TCC is the measure of ε_r variation relative to that at room temperature in a given temperature range. For PIs, the TCC can be as high as −15% from room temperature to 300°C, where the minus sign indicates that the ε_r of PI decreases with increasing temperature. Variations in dielectric constant are undesirable for most capacitor applications, especially for

power conditioning, filtering, timing, and tuning circuitries. PEIs also show a considerable TCC of ~6% from room temperature to 200°C.

3.1.2. Fluorene polyester and cross-linked divinyltetramethyldisiloxane-bis(benzocyclobutene). Fluorene polyesters (FPEs) and cross-linked divinyltetramethyldisiloxane-bis(benzocyclobutenes) (*c*-BCBs), with a similar grade of thermal stability as PIs, offer superior dielectric stability versus temperature. FPEs (T_g = 330°C) represent a class of amorphous polyarylates prepared through the reaction of fluorene bisphenol with phthalic chlorides. Pristine FPE shows a TCC exceeding 8% (37), but for chemically modified FPE, referred to as FDAPE (50), the TCC is less than 1% in the temperature range of 25–350°C, and the dissipation factor of FDAPE is constantly lower than 0.4% in the same temperature span. This makes FDAPE an excellent dielectric for high-temperature power conditioning applications, in which a high dielectric stability with temperature is required. Moreover, at 150°C, the maximum dischargeable energy density of FPE is ~1.2 J/cm^3 (achieved at 350 MV/m), which is twice as high as that of Kapton (37) (**Figure 3**).

As thermoset dielectric polymers, *c*-BCBs are thermally cross-linked or photo-cross-linked from the BCB monomer through a 4 + 2 Diels–Alder reaction, i.e., an intermolecular reaction between the alkene unit and the *o*-quinodimethane intermediate from ring opening of the benzocyclobutene (51). These materials are available in both monomer and *b*-staged (partially polymerized) forms from commercial sources such as cyclotene resins by Dow Chemicals. Fully cured *c*-BCBs possess an ε_r of ~2.7 and a dissipation factor of ~0.15% at room temperature and 1 kHz, and such values remain almost constant up to 300°C and 2 MHz (37). The TCC of *c*-BCBs is approximately −2.4% in the temperature range of 25–350°C (37). While *c*-BCBs undergo no glass transition before thermally decomposing (>350°C) (37), they are sensitive to oxygen at elevated temperatures because of the oxidation of benzylic CH_2 groups to anhydride and/or carbonyl species (52). This event in turn leads to weight loss over time at temperatures above 300°C. Modified formulations of *c*-BCBs have been successfully developed to reduce the sensitivity to oxidation (53).

3.1.3. Polycarbonate and poly(phenylene sulfide). High-quality PIs, FPEs, and *c*-BCBs have excellent thermal resistance but are expensive. For lower requirements of temperature capability, polymer dielectrics with compromised thermal stability but lower price are of higher interest for practical applications. Polycarbonate (PC) is a dielectric polymer synthesized from carbonic acids and dihydric alcohols. The temperature rating of PCs is limited to approximately 150°C by its T_g. The advantage of PCs for high-temperature film capacitor applications is their dielectric stability over temperature, i.e., a low TCC value of approximately −3% (37). After the discontinuation of capacitor PC films by the main supplier, Bayer AG, at the end of 2000, most manufacturers ceased their production of PC film capacitors (54). Poly(phenylene sulfides) (PPSs), consisting of aromatic rings linked with sulfides, are considered an ideal replacement for PC films in high-temperature capacitor applications on account of their very similar dielectric properties, including a low dissipation factor and decent dielectric stability with temperature. Although PPSs have a low T_g (~120°C) relative to other high-temperature polymer dielectrics, they can be rated at 150°C or even 200°C for film capacitor applications (55). TORELINA® is a trade name given to a commercialized PPS film manufactured by Toray Industries. The TCC of TORELINA films is only approximately 1.5% within the projected operating temperature range, and the dissipation factor stays at an extremely low level (below 0.1% at 1 kHz) until the temperature increases to above 100°C (still below 0.5% up to 150°C). However, reports on high-temperature energy storage performance of PPSs are rare.

Annu. Rev. Mater. Res. 2018.48:219-243. Downloaded from www.annualreviews.org
Access provided by Copenhagen University on 05/07/22. For personal use only.

3.1.4. Polyketone. Polyketones are a series of polymers containing ketone groups in the backbone. Poly(ether ether ketone) (PEEK) is one of the most important members of the polyketone family. PEEKs can be readily polymerized from the dialkylation of bisphenolate salts. Commercialized PEEKs are available from multiple sources such as Solvay and Victrex. For example, Ketaspire® PEEK film by Solvay is characterized by a T_g of 150°C. The dissipation factor of PEEKs increases rapidly above 150°C. At 150°C, PEEK delivers an energy density of ~0.5 J/cm^3 at a low efficiency of 55% at 200 MV/m (37) (**Figure 3**). The physical properties of polyketone materials are tunable by varying the ether:ketone group ratio, which results in materials analogous to PEEKs. For instance, poly(ether ketone ketone) (PEKK) has a chemical structure similar to that of PEEKs; i.e., the mole ratio of ether group to ketone group in PEKKs is 1:2, while that in PEEKs is 2:1. PEKKs are synthesized via a reaction between diphenyl ether and a mixture of benzene dicarboxylic acid halides (56). PEKKs are usually a copolymer of terephthalic (T) moieties and isophthalic (I) moieties, and the T:I ratio determines the main physical properties of the resultant PEKKs. The T_m and T_g of PEKKs vary between 305°C and 360°C and between 160°C and 165°C, respectively, with changing T:I ratio. Kepstan® by Arkema is a commercialized PEKK copolymer with a T_g of 162°C. This PEKK is able to discharge an energy density of ~0.6 J/cm^3 with an efficiency of 90% under an electric field of 200 MV/m and at 160°C (57). This performance is among the best in all the high-temperature polymer dielectrics under comparable conditions. The incorporation of the rigid asymmetric phenyl phthalazinone moiety into the polyketone backbone yields poly(phthalazinone ether ketone) (PPEK) with a T_g of 250°C. PPEK displays excellent stability in dielectric properties over a broad frequency and temperature range. Little change in the breakdown field (~440 MV/m) and discharge time has been observed in PPEK with an increase of temperature up to 190°C (58).

3.2. Polymer Nanocomposites

The polymer composite approach to dielectric materials combines the unique thermal, mechanical, and electrical properties of inorganic inclusions with the facile processability and high breakdown strength of polymeric matrices for improved dielectric properties and capacitive energy storage performance (27, 29, 59–61).

3.2.1. Single-layer composites. Incorporation of inorganic dopants creates interfacial interaction and physical confinement on the polymer dielectric and thus drives T_g (62, 63) toward higher values. For example, PEIs filled with 5 wt% of sepiolite [i.e., hydrated magnesium silicate with the half-unit-cell formula of $Mg_8Si_{12}O_{30}(OH)_4{\cdot}12H_2O$] needles have an improved T_g (i.e., 223°C) relative to the bare polymer, which has a T_g of 215°C (64). Moreover, high-aspect-ratio dopants commonly reinforce the mechanical properties of polymer materials (65–68). The reinforcement of mechanical properties could, in principle, result in much improved dielectric breakdown strength in polymer nanocomposites since the electromechanical breakdown model is dominant for low-modulus materials (69). However, invariably particles lead to a decreased Weibull modulus of the breakdown field. This effect is even more pronounced under elevated-temperature conditions because polymers usually soften with increasing temperature; e.g., *c*-BCBs filled with 10 vol% of boron nitride nanosheets (BNNSs) show an ~50% increase in Weibull breakdown strength at 250°C (37).

Aside from improving the mechanical properties of polymers, there is the possibility of using suitably oriented high-aspect-ratio fillers to enhance the insulating properties of polymer dielectrics. The enhancement in insulating properties is usually correlated with one of the following

Annu. Rev. Mater. Res. 2018.48:219-243. Downloaded from www.annualreviews.org
Access provided by Copenhagen University on 05/07/22. For personal use only.

three phenomena but remains to be established. First, the introduction of a second phase augments the path length of carriers responsible for electrical conduction (70). Second, phase-field modeling indicates that high-aspect-ratio fillers are favorable for mitigating local field concentration (71, 72). Third, high-aspect-ratio nanofillers can provide resistance to electric treeing inception (73). Li et al. (37) reported that the leakage current density of BNNS-filled *c*-BCB is more than an order of magnitude less than that of the pristine *c*-BCB. As such, *c*-BCB/BNNS outperforms all previous high-temperature polymer dielectrics in terms of high-temperature energy storage capability (**Figure 3**). For example, under an electric field of 200 MV/m and at 150°C, the conduction loss of *c*-BCB/BNNS is merely 3%.

Some high-aspect-ratio fillers, e.g., boron nitride, have both excellent insulating properties and high thermal conductivity. Among the many allotropes of boron nitride, hexagonal BNNSs and boron nitride nanotubes are the most attractive, given their high efficiency in heat transport in polymer matrix (74). Due to the significantly improved thermal conductivity and much decreased leakage current of polymer dielectrics, their thermal runaway under elevated-temperature conditions is suppressed (37). Furthermore, inorganic fillers with high ε_r are doped in polymer dielectric to increase the overall permittivity and hence the capacitance and energy storage densities (27–29, 75–77). For example, PIs loaded with 30 vol% of barium titanate fibers exhibit an ε_r as high as 27—almost an order of magnitude higher than that of the pristine polymer—in addition to a relatively low dissipation factor of 1.5% (77).

3.2.2. Sandwich-structured composites. The single-layered composite approach to high ε_r generally results in dramatically reduced breakdown strength owing to the local field distortion (29). To bypass this issue, sandwich-structured composites have been developed (78–80). The main idea is to create spatially organized dielectric hard (low-ε_r) and dielectric soft (high-ε_r) layers to rearrange the distribution of the electric field. The effective and strong barrier interfaces that exist between adjacent layers in the sandwich structure protect the composite films from total breakdown and suppress the formation of conductive paths in the hard layer, while high polarization induced by the barium titanate (BT) nanoparticles in soft layers guarantees a high dielectric maximum polarization. Further improvements in the breakdown strength and energy density have been realized for a group of three-tiered ferroelectric poly(vinylidene fluoride) films with an increase in BT content in a layer-by-layer gradient (81).

For high-temperature applications, however, to simply mitigate the field concentration does not solve all the problems, as the main issue is the significant conduction loss associated with thermally activated charge carriers. In this regard, a sandwich-structured polymer nanocomposite with BNNSs spreading throughout the outer polymeric layers and high-ε_r nanoparticles in the interior layer has been rationally designed and experimentally demonstrated (10, 82) (**Figure 4**). BNNSs serve not only as scattering centers to the migration of charge carriers but also as barriers against the thermionic charge injection that is a main source of conduction loss at elevated temperatures. With *c*-BCB as the polymeric matrix, this configuration has led to the highest value of energy density at 150°C (i.e., 4 J/cm^3) in polymer-based dielectrics reported thus far (10) (**Figure 4**). More recently, chemical-vapor-deposited hexagonal boron nitride (*h*-BN) with controlled thickness was successfully transferred from a copper foil to the surface of PEI films (83) (**Figure 5**). The *h*-BN-coated PEI films are capable of operating with >90% efficiencies and delivering high energy densities, i.e., 1.2 J/cm^3, even at a temperature close to the T_g of polymer (i.e., 217°C), at which pristine PEI almost fails. Outstanding cyclability and dielectric stability over 55,000 continuous charge-discharge cycles have been demonstrated in *h*-BN-coated PEI at high temperatures.

Annu. Rev. Mater. Res. 2018.48:219-243. Downloaded from www.annualreviews.org
Access provided by Copenhagen University on 05/07/22. For personal use only.

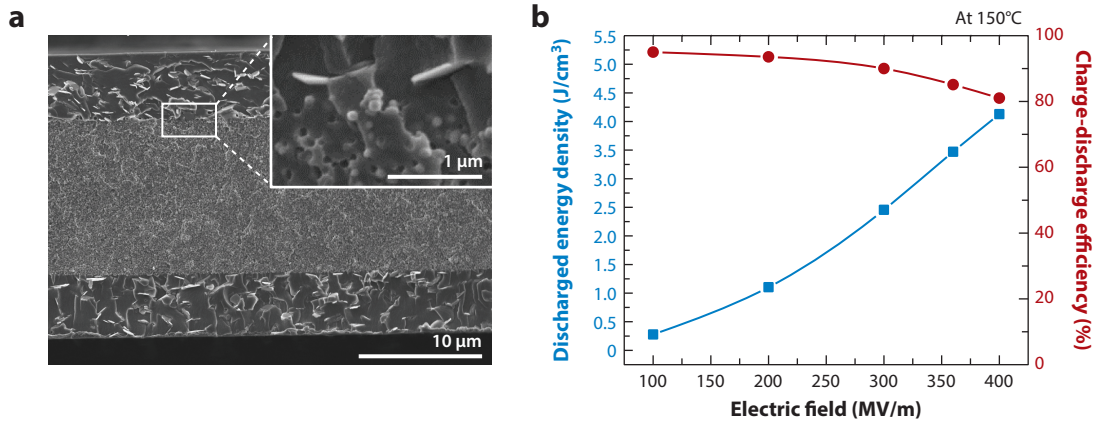

Figure 4

(*a*) Cross-sectional SEM image and (*b*) energy storage performance of sandwich-structured nanocomposites measured at 150°C. Reprinted with permission from Reference 10. Copyright © 2016, National Academy of Sciences of the United States of America.

3.3. High-Temperature Inorganic Dielectrics

In parallel with the advancements in high-temperature polymer dielectrics, significant developments have been made in inorganic dielectric materials, which can be categorized into four groups, namely inorganic film, ceramic, glass, and ceramic-glass composites. Although the ambient figures of merit of inorganic dielectrics have been reviewed (84, 85), recent progress in high-temperature inorganic dielectrics remains to be summarized and is addressed in the following sections, with an emphasis on inorganic films and ceramics.

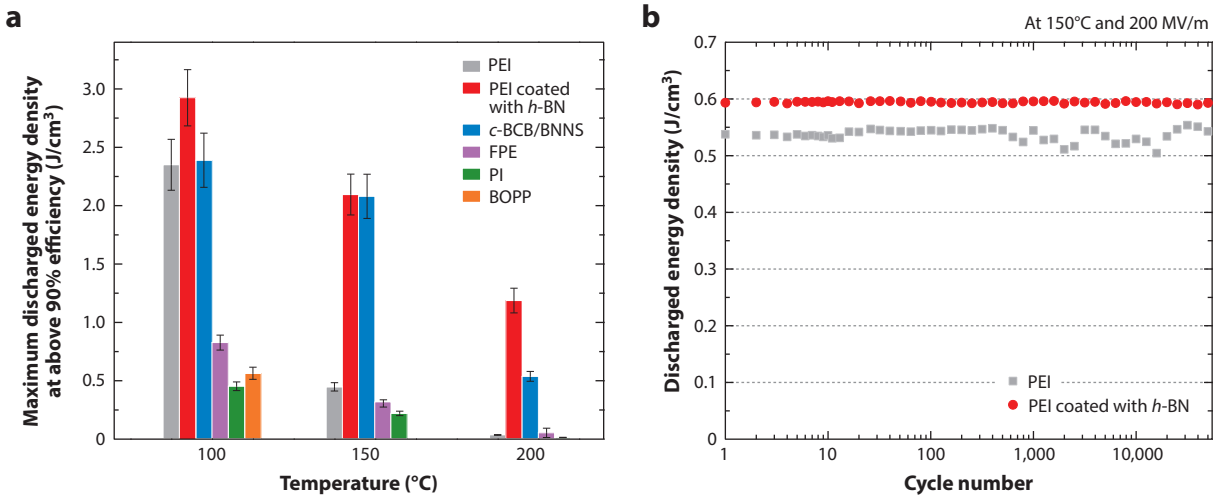

Figure 5

(*a*) Maximum discharged energy density at above 90% charge-discharge efficiency of polymers and polymer nanocomposites. (*b*) Cyclic performance of PEI film coated with boron nitride at 150°C. Abbreviations: BOPP, biaxially oriented polypropylene; *c*-BCB/BNNS, cross-linked divinyltetramethyldisiloxane-bis(benzocyclobutene)/boron nitride nanosheet; FPE, fluorene polyester; *h*-BN, hexagonal boron nitride; PEI, poly(ether imide); PI, polyimide. Reprinted with permission from Reference 83. Copyright © 2017, Wiley-VCH.

Annu. Rev. Mater. Res. 2018.48:219-243. Downloaded from www.annualreviews.org
Access provided by Copenhagen University on 05/07/22. For personal use only.

3.3.1. Main material systems. There are four classical dielectrics for energy storage: linear dielectric, ferroelectric, relaxor ferroelectric, and antiferroelectric materials. Linear dielectric ceramics, which have relatively low dielectric constant, low dielectric loss, and high dielectric breakdown strength, are of great potential for high-temperature energy storage applications. The representative high-temperature linear dielectrics are perovskite $CaTiO_3$- and $CaZrO_3$-based solid solutions. Incipient ferroelectric $CaTiO_3$ has a relatively high permittivity of approximately 171, while $CaZrO_3$ is an interesting material with a large bandgap of 4.0–5.5 eV. Therefore, solid solutions of $CaTiO_3$ and $CaZrO_3$ are promising materials for high-temperature applications. $Ca(Zr_{0.8}Ti_{0.2})O_3$ ceramics are reported to have a permittivity of 43 at room temperature and a low TCC of −0.03% over the temperature range from 25°C to 250°C. $Ca(Zr_{0.8}Ti_{0.2})O_3$ capacitors show a high energy density of 2.49 J/cm^3 and 4.19 J/cm^3 at 25°C and 250°C, respectively (86). However, the low permittivity of $CaZrO_3$ limits improvements in energy storage performance. Subsequently, high-permittivity $CaTiO_3$ modified by $CaHfO_3$, which has a higher bandgap (∼6.4 eV) than does $CaZrO_3$, has been investigated. $Ca(Ti_{0.8}Hf_{0.2})O_3$ (CHT) capacitors yield an ambient energy density as high as 9.0 J/cm^3 but show a drastic decrease in energy density above 100°C. Mn doping could effectively mitigate high temperature and high field losses of CHT capacitors, resulting in an energy storage density that is similar to that of ambient values (∼9.5 J/cm^3) up to 200°C and that remains high (6.5 J/cm^3) even at 300°C (87). The design rationale here lies in developing materials with large bandgap, linear or weakly nonlinear permittivity, and high breakdown strength. Thus, there is enormous experimental design space for high-temperature linear dielectric materials such as $BaZrO_3$-$CaTiO_3$ and $SrZrO_3$-$CaTiO_3$ (88).

In contrast to linear dielectrics, ferroelectrics exhibit nonlinear hysteresis, moderate electric breakdown strength, and high saturated polarization but low energy storage density and efficiency as a result of high remnant polarization and hysteresis. Fortunately, relaxor ferroelectrics inherit the advantages of typical ferroelectrics such as high saturated polarization but have dramatically reduced remnant polarization and hysteresis relative to other ferroelectrics, which make relaxor ferroelectrics good candidates in the search for high-temperature inorganic dielectrics for energy storage. Lead-based relaxor ferroelectric films have recently attracted increasing attention, particularly since a high energy storage density of 85 J/cm^3 was reported for (Pb,La)(Zr,Ti)O_3 (PLZT) relaxor ferroelectric films (89). Tong et al. (90) reported the temperature dependence of energy storage properties of polycrystalline PLZT relaxor ferroelectric films deposited on nickel buffered by a lanthanum nickel oxide buffer layer. The energy density and efficiency are almost temperature independent and remain constant, at 25 J/cm^3 and 70%, respectively, in the temperature range of 20°C to 200°C (measured at 200 MV/m). Beyond the PLZT system, high-temperature piezoelectric materials are screened as potential alternatives for energy storage, as exemplified by $Bi(Na_{1/2}Hf_{1/2})O_3$-$PbTiO_3$ (BNH-PT) solid solutions, which have the inherent advantages of high Curie temperature and strong relaxor behavior (91).

Driven by the ever-increasing concerns regarding environmental sustainability, recent advances in high-temperature dielectrics have also occurred for lead-free relaxor ferroelectrics, primarily bismuth-based compounds, such as (Bi,Na)TiO_3 and $Bi(Me^{3+})O_3$ (Me can be either a single trivalent cation or two cations with an average of +3 valence that occupy the octahedral sites) and their derivatives (92–101). $(Bi_{1/2}Na_{1/2})_{0.9118}La_{0.02}Ba_{0.0582}(Ti_{0.97}Zr_{0.03})O_3$ epitaxial lead-free relaxor thin films with coexisting ferroelectric and antiferroelectric phases can withstand a unipolar electric field up to 350 MV/m, yielding a high energy density of 154 J/cm^3 with an efficiency of 97%, and the energy density fluctuates slightly from room temperature to 250°C (94). Solid solutions of bismuth-based compounds with $BaTiO_3$ are of great interest because the phase transition of complex perovskites can be compositionally manipulated to engineer the temperature dependence of dielectric properties. Recent work by Kwon & Lee (102) unveiled the weakly coupled

Annu. Rev. Mater. Res. 2018.48:219-243. Downloaded from www.annualreviews.org
Access provided by Copenhagen University on 05/07/22. For personal use only.

relaxor behavior of $BaTiO_3$-$Bi(Mg,Ti)O_3$ thin films. These films present a nearly linear polarization response, with a high permittivity exceeding 900 and a breakdown strength of 208 MV/m, contributing to a high energy density of 37 J/cm^3. Of particular significance is the fact that the dielectric permittivity and energy storage properties can be maintained at high temperatures up to 200°C. $BaTiO_3$/$SrTiO_3$-substituted $BiFeO_3$, a multiferroelectric with high intrinsic polarization and high Curie temperature, also exhibits strong relaxor behavior and temperature-insensitive permittivity over a broad temperature range, showing potential for high-temperature dielectric capacitors (95, 103, 104). For example, a high energy density of 51 J/cm^3 at a field of 350 MV/m was experimentally reported for Mn-doped $0.4BiFeO_3$-$0.6SrTiO_3$ relaxor ferroelectric thin films, accompanied by decent resistance against thermal stimulation and electrical cycling (95). Most research on $(Bi,Na)TiO_3$-based lead-free ceramics focuses on exploring the transition between ergodic and nonergodic relaxor phases by incorporating a second or even a third component to optimize energy storage performance. For instance, $Bi_{0.5}Na_{0.5}TiO_3$ ceramics comodified by $BaTiO_3$ and $K_{0.5}Na_{0.5}NbO_3$ show temperature-insensitive permittivity up to 300°C (normalized permittivity $\varepsilon/\varepsilon_{150°C}$ varies no more than ±10% from 43°C to 319°C), although at the expense of a small reduction in permittivity (96). Ceramics with the composition $0.76Bi_{0.5}Na_{0.5}TiO_3$-$0.19SrTiO_3$-$0.05NaNbO_3$ are endowed with a nearly temperature-invariant recoverable energy density of 0.6 J/cm^3 from 25°C to 160°C within the ergodic region (97).

Antiferroelectrics characterized by double hysteresis are considered to be promising candidates for electrostatic energy storage; $PbZrO_3$-based antiferroelectrics in particular have attracted much attention. Similar to other ABO_3-type perovskites, $PbZrO_3$ has been extensively modified with isovalent additives (such as Sr or Ba in *A* sites and Ti or Sn in *B* sites) and/or off-valence additives (such as La in *A* sites) to strengthen its performance (105–108). For instance, the synergistic effects of composition optimization and strain engineering endow textured PLZT antiferroelectric films with excellent thermal stability, where a high recoverable energy storage density of 20 J/cm^3 and an efficiency above 60% are nearly independent of temperature up to 280°C (at 160 MV/m), as shown in **Figure 6** (108). Researchers retain a keen interest in exploring new lead-free systems for high-temperature electrostatic capacitors. HfO_2-based thin films emerge as promising candidates. HfO_2 with various dopants, such as Si, Al, and Zr, was reported to be a ferroelectric or an

Annu. Rev. Mater. Res. 2018.48:219-243. Downloaded from www.annualreviews.org
Access provided by Copenhagen University on 05/07/22. For personal use only.

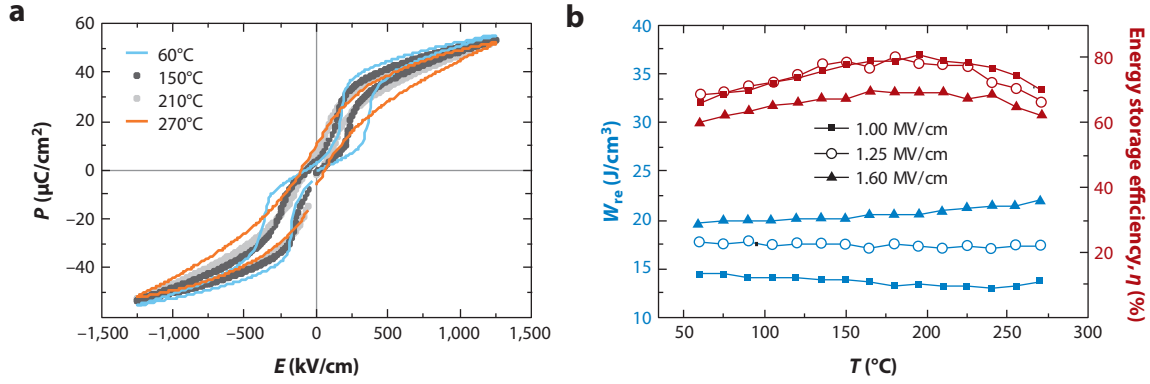

Figure 6

(*a*) Representative hysteresis at different temperatures and (*b*) temperature dependence of energy storage density (W_{re}) and energy storage efficiency (η) for $(Pb,La)(Zr,Ti)O_3$ 2/95/5 thick films. Abbreviations: *E*, electric field; *P*, polarization; *T*, temperature. Reprinted with permission from Reference 108. Copyright © 2016, AIP Publishing LLC.

antiferroelectric material. In particular, Zr-doped HfO_2 has a much higher bandgap (5.5 eV) than does $Pb(Zr,Ti)O_3$ (3.0 eV), which ensures a higher breakdown strength. Experiments have confirmed that the breakdown field and energy storage density of $Hf_{0.3}Zr_{0.7}O_2$ antiferroelectric thin films prepared using atomic layer deposition are as high as 435 MV/m and 45 J/cm^3, respectively (109). Equally important features are robust thermal stability up to 175°C and fatigue resistance up to 10^9 times of electrical cycling (109). Lead-free antiferroelectric ceramics, primarily the niobates, have also attracted great attention for high-temperature energy storage applications. Despite the debates on the ferroelectric or antiferroelectric characteristics of $NaNbO_3$, lowering the tolerance factor could credibly stabilize the antiferroelectricity in $NaNbO_3$ through chemical modification (110–112). As an analog of $NaNbO_3$, lead-free $AgNbO_3$ antiferroelectric ceramics show a peak recoverable energy density of 1.6 J/cm^3 at 14 MV/m (113). Tantalum-modified $AgNbO_3$ has enhanced antiferroelectricity and increased dielectric breakdown strength, due to the reduced polarizability of *B*-site cations and increased bulk density, respectively, yielding significantly enhanced performance, with an energy density of 4.2 J/cm^3 and high thermal stability of energy density (minimal variation of $<\pm 5\%$) over a broad temperature range (114).

3.3.2. Synthetic approach. The emerging advanced approaches to material synthesis benefit the development of high-end inorganic dielectrics. PLZT-based antiferroelectric ceramics prepared through the conventional solid-state sintering (CS) method possess (*a*) low energy storage density (<1.5 J/cm^3) because of defect-induced low dielectric breakdown strength and (*b*) poor thermal stability originating from the destabilized antiferroelectricity at high temperatures approaching the Curie point (115–117). To address these issues, spark plasma sintering (SPS), an advanced sintering technique, was employed to deliver high-performance antiferroelectric composite ceramics $(Pb_{0.858}Ba_{0.1}La_{0.02}Y_{0.008})(Zr_{0.65}Sn_{0.3}Ti_{0.05})O_3$-$(Pb_{0.97}La_{0.02})(Zr_{0.9}Sn_{0.05}Ti_{0.05})O_3$ (PBLYZST-PLZST) (118, 119). In contrast to the CS process, SPS—with the advantages of low sintering temperature, short soaking durance, and a stress-assisted densification process—could strongly suppress diffusion between tetragonal antiferroelectric PBLYZST and orthorhombic antiferroelectric PLZST. In consequence, both a considerably high ferroelectric-to-antiferroelectric phase transition field of 16.2 MV/m and improved temperature stability of orthorhombic antiferroelectricity contributed by the tetragonal PBLYZST phase were obtained. PBLYZST-PLZST composite ceramics that underwent SPS showed a high recoverable energy density of 6.4 J/cm^3 and excellent thermal stability of energy storage density of 1.16×10^{-2} J/(°C·cm^3); this energy density and its thermal stability were much superior to those of samples that underwent CS (118, 119). Nonetheless, the SPS technique may be more suitable for the laboratory scale rather than for mass production, given the lower degrees of freedom and the higher cost for SPS processing relative to CS processing.

3.3.3. Defect engineering and microstructure control. The influence of defects, such as oxygen vacancies and grain boundaries, cannot be overlooked in inorganic dielectrics. Defects are double edged, as they can be harmful to the electrical properties of materials but can also be manipulated to boost performance. Thus, there are two options for achieving superior energy storage properties: lowering the concentration of defects or making the best of them. For example, Hu et al. (120) prepared high-quality epitaxial PLZT relaxor ferroelectric thin films by using pulsed laser deposition. In contrast to the polycrystalline counterparts, epitaxial PLZT films have a reduced number of defects and grain boundaries, showing a significantly enhanced breakdown strength of 227 MV/m and an energy storage density of 31 J/cm^3. Moreover, the high energy storage density is negligibly temperature dependent over a wide temperature range from 20°C to 180°C. In contrast, an off-valence additive (Mn) was deliberately incorporated into PLZT relaxor

Annu. Rev. Mater. Res. 2018.48:219-243. Downloaded from www.annualreviews.org
Access provided by Copenhagen University on 05/07/22. For personal use only.

ferroelectric thin films to form a defect complex between Mn and oxygen vacancies (121). The defect complex can be oriented along the direction of the external field, contributing to improved dielectric and ferroelectric properties. Moreover, the concentration of oxygen vacancies can be reduced, and such reduction is advantageous for higher breakdown strength. Accordingly, Mn-doped PLZT relaxor ferroelectric films have superior energy storage behavior. Consistent results also occur in Mn-incorporated $0.4BiFeO_3$-$0.6SrTiO_3$ relaxor ferroelectric thin films (95) and $AgNbO_3$ lead-free antiferroelectric ceramics (113).

3.3.4. Multilayer structure and interface effect. Rational configuration design can be an effective approach to explore dielectrics with desirable energy storage performance, such as layered structures (122–124) and superlattices (125), given the significance of interfaces in ferroelectric/dielectric multilayers or superlattices. Zhao et al. (123) found that compositionally graded multilayer PLZT antiferroelectric thick films exhibit significantly enhanced dielectric properties and energy storage performance, particularly for upgraded films, and such improvements were attributed to the strain and gradient of polarization near the interfaces of adjacent layers. The energy density varies slightly from 19.2 to 17.9 J/cm^3, and an efficiency of approximately 76% is maintained over the temperature range of 20°C to 150°C. Sun et al. (124) devised $(Ba_{0.7}Ca_{0.3}TiO_3/BaZr_{0.2}Ti_{0.8}O_3)_N$ ($N = 2$, 4, 8) multilayer structures by the magnetron sputtering technique (**Figure 7*a–c***). The interfaces effectively impede the development of electric trees (**Figure 7*d–f***), leading to a remarkable increase in breakdown strength (**Figure 7*g***). Multilayers with $N = 8$ possess an extraordinary breakdown strength of 470 MV/m. Hence, a superior energy storage density of 52.4 J/cm^3 with a high efficiency of 72.3% was recorded at 450 MV/m (**Figure 7*h***). Most importantly, the $N = 4$ multilayers present excellent thermal stability with an energy density of 34.8 J/cm^3 and an efficiency of 75.1% over a wide temperature range from 25°C to 140°C (**Figure 7*i***), representing the benchmark in lead-free thin films for high-temperature dielectric capacitors.

3.3.5. Prototyped devices. For dielectric ceramics, making complex devices by using these materials in the form of multilayers is essential. Single-layer capacitors were prototyped to confirm the feasibility of $0.3BiScO_3$-$0.7BaTiO_3$ ceramics, which have a high and temperature-stable dielectric constant (~1,000 up to 300°C) coupled with a high electrical resistivity (~10^{12} Ω · m at 250°C), for applications in high-energy density capacitors operating at elevated temperature (99). The ambient energy density of the thin dielectric layer capacitors is as high as 6.1 J/cm^3 at a field of 73 MV/m. Another attractive aspect is that these capacitors exhibit decent thermal stability up to 300°C with a relatively high energy density value of approximately 3.0 J/cm^3 at 37 MV/m (99). The comprehensive performance of $0.3BiScO_3$-$0.7BaTiO_3$ capacitors is comparable to or even surpasses that of commercial capacitors, including NP0, base metal electrode X7R, and precious metal electrode X7R (98). Correia et al. (126) demonstrated that low self-heating (reduced losses), high energy density (2.7 J/cm^3 at 32 MV/m), and good thermal stability (with energy density varying by less than 18% over the temperature range 20–200°C) allow $0.2BiFeO_3$-$0.8SrTiO_3$ multilayer capacitors to be viable high-temperature pulsed power devices.

4. CHALLENGES, OPPORTUNITIES, AND FUTURE PROSPECTS

The availability of high-temperature dielectrics is key to the development of advanced electronic and electrical power systems operating under extreme environment conditions. There have been many exciting developments over the past several years. The currently available material candidates and approaches, however, still fall short of the desired specifications, and there is plenty of room for further improvement, as several issues remain to be addressed. Future development of

Annu. Rev. Mater. Res. 2018.48:219-243. Downloaded from www.annualreviews.org
Access provided by Copenhagen University on 05/07/22. For personal use only.

Annu. Rev. Mater. Res. 2018.48:219-243. Downloaded from www.annualreviews.org
Access provided by Copenhagen University on 05/07/22. For personal use only.

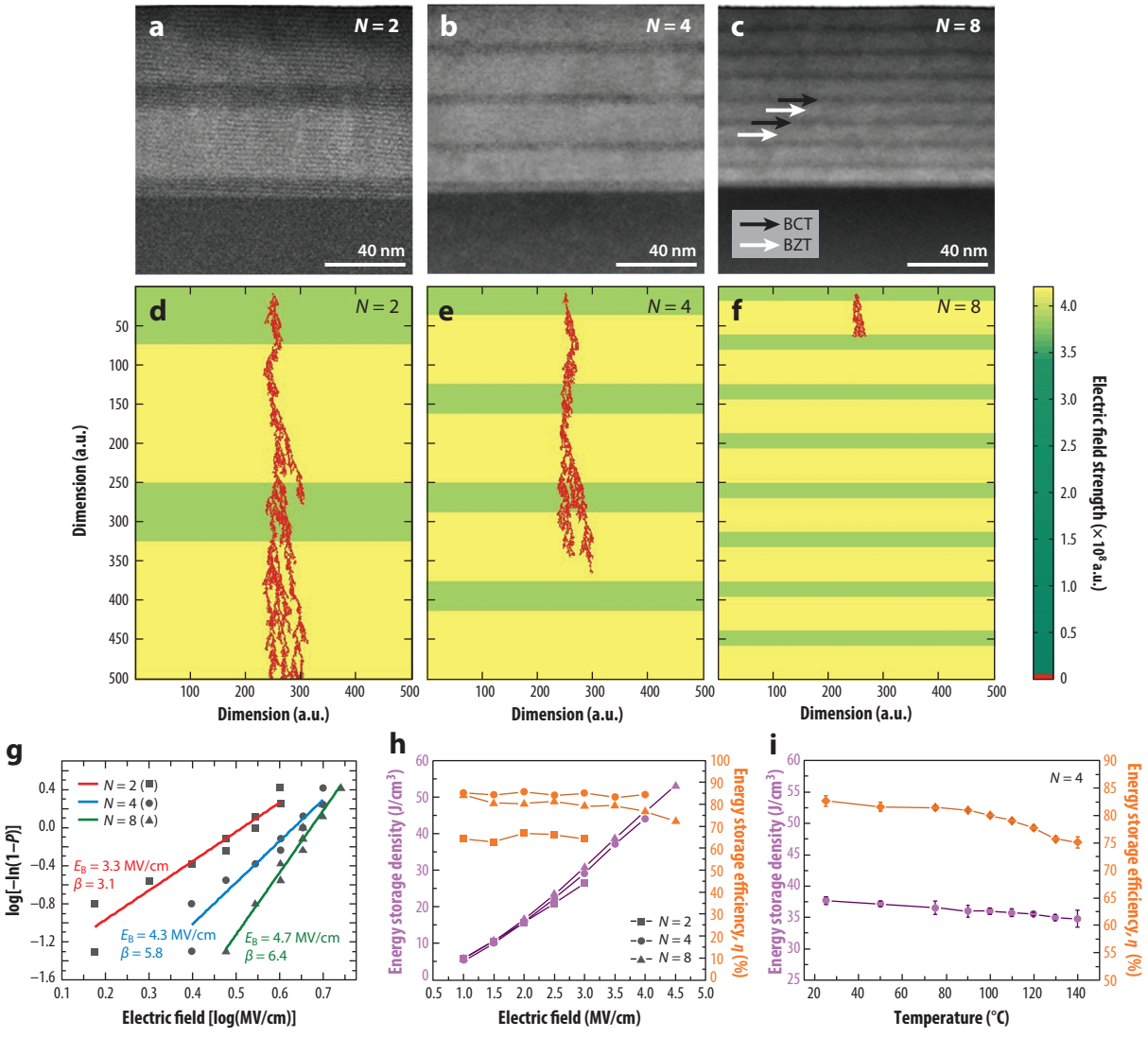

Figure 7

(*a–c*) Cross-sectional STEM images and (*d–f*) simulated development of electric trees in $Ba_{0.7}Ca_{0.3}TiO_3/BaZr_{0.2}Ti_{0.8}O_3$ (BCT/BZT) multilayers with $N = 2, 4, 8$. (*g*) Weibull distribution for the dielectric breakdown strength E_B. β is the shape parameter indicating the dispersion of the experimental data. (*b*,*i*) Dependence of energy density and efficiency on (*b*) electric field and (*i*) temperature for the BCT/BZT multilayers. Reprinted with permission from Reference 124. Copyright © 2017, Wiley-VCH.

high-temperature dielectrics should combine, for example, an improved fundamental understanding, rational design of materials, and scalable synthesis and processing approaches. In this context, challenges and opportunities may include, but are not limited to, the following aspects.

To attain high thermal resistance and hence good dielectric stability at elevated temperatures, most high-temperature polymer dielectrics contain aromatic or heteroaromatic molecular units in the backbone. But these electronically conjugated structures may have adverse effects on the insulating properties of polymer dielectrics in that they introduce impurity states into the energy

bandgap (127). Another issue associated with the presence of aromatic or heteroaromatic molecular units is the possible impact on the self-clearing capability of metallized film capacitors. In some cases, e.g., in metallized PIs and PPSs, traces of carbon may remain in the area when the defect site is burned out (when clearing occurs), which results in poor electrical properties. As such, new molecular design of the skeleton structure of dielectric polymers should be performed to balance the dimensional and thermal stability and to perfect insulating properties. A systematic study of polymer structure versus high-temperature high-field dielectric performance has not yet been carried out.

Under both high temperatures and high electric fields, the conduction loss of polymer materials is significant. For instance, while the weak-field dissipation factor of Kapton is below 0.1% at 150°C, under an electric field of 200 MV/m, the conduction loss is as high as 24%. The dissipated energy manifests as Joule heat and may cause thermal runaway of the device. The energy dissipation is associated with various temperature- and field-dependent conduction events such as thermionic and thermionic-field charge injections, Poole-Frenkel emission, hopping, and tunneling. To suppress these conduction events, a high-energy barrier at the electrode-dielectric interface and deep energy traps in the material bulk may need to be developed. To this end, surface functionalization as well as molecular engineering in polymer dielectric films should be considered. Deep traps can be generated via incorporation of inorganic units into polymers to form organic-inorganic hybrid and composite structures (128).

The current high-temperature polymer dielectrics possess relatively low ε_r values, i.e., below 4, which severely limit the energy storage density and leave a large footprint of film capacitors in electronic devices and power systems. The various forms of loss associated with conventional approaches for permittivity lifting are unacceptably high for high-temperature film capacitor applications. To address this issue, topological structure engineering of composite systems and judicious molecular modification have been carried out, and both show promise for high-permittivity and low-loss materials, especially at elevated temperatures and high fields. But this specific area of study is still in its infancy, and large-scale production of these new materials remains a challenge. Much research still remains to understand the complex structure-property relationships, e.g., the polarity of functional groups versus dielectric permittivity/loss under conditions of elevated temperatures and high applied electric fields.

Thermal conductivity is also a limiting factor for high-temperature polymer dielectric materials because the operating temperature is determined by the ability to conduct out heat. However, polymers have relatively low thermal conductivities, with very few exceptions. A strategy capitalizing on engineered interchain interactions very recently resulted in amorphous polymer blends with high thermal conductivities up to 1.5 W/(m·K) (129). This strategy is expected to be extended to high-temperature polymer dielectric materials. Moreover, composite approaches are well known for being able to improve the thermal conductivity of polymer dielectrics, given the existence of various types of nanofillers with high thermal conductivities and decent insulating properties. The realization of this strategy depends on the nanomorphology of the fillers as well as on the spatial organization of the nanofillers in the polymer matrix.

For inorganic dielectrics, intrinsically, the synergistic effects of large bandgap and high polarization are advantageous; extrinsically, multiscale structures—ranging from atomic-scale defects, to nanoscale structures such as polar nanoregions in relaxor ferroelectrics, to micro/macrostructure design such as that involving multilayers—play a crucial role in tailoring the energy storage properties. Thus, enormous experimental design space still remains for high-temperature inorganic dielectric materials.

Wafer-scale inorganic films prepared by facile approaches with homogeneous composition and microstructure and decent comprehensive energy storage properties are desired for practical applications. As our ability to produce high-quality materials and integrate them into novel

Annu. Rev. Mater. Res. 2018.48:219-243. Downloaded from www.annualreviews.org
Access provided by Copenhagen University on 05/07/22. For personal use only.

structures improves, production of free-standing inorganic dielectric films opens the way to multifunctional devices. For dielectric ceramics, mass production of multilayered ceramic capacitors is demanded for practical uses. Effort should be paid to rational device design strategies, such as structure design, to optimize the performance of capacitors. The compatibility of ceramics with internal electrodes, particularly low-cost metals (e.g., nickel), should also be considered.

In conclusion, we are witnessing groundbreaking developments in materials science. It is to be expected that these developments, coupled with recent major developments in high-performance polymers and electroactive ceramics and ongoing fundamental research on dielectric phenomena, should lead to the development of scalable, high-performance dielectric materials that will revolutionize energy storage devices built for harsh environments.

DISCLOSURE STATEMENT

The authors are not aware of any affiliations, memberships, funding, or financial holdings that might be perceived as affecting the objectivity of this review.

ACKNOWLEDGMENTS

The work was supported by the US Office of Naval Research (QW), by National Natural Science Foundation of China (grant 51777101) and self-determined research funds of the State Key Laboratory of Control and Simulation of Power System and Generation Equipments (SKLD17M07) (QL), and by the National Key Research Program of China (2015CB654603 and 2017YFB0406303) (HW). F-ZY acknowledges the China Postdoctoral Science Foundation for support (2016M602812).

LITERATURE CITED

1. Sarjeant WJ, Zirnheld J, MacDougall FW. 1998. Capacitors. *IEEE Trans. Plasma Sci.* 26:1368–92
2. Irvine JTS, Sinclair DC, West AR. 1990. Electroceramics: characterization by impedance spectroscopy. *Adv. Mater.* 2:132–38
3. Sarjeant WJ, Clelland IW, Price RA. 2001. Capacitive components for power electronics. *Proc. IEEE* 89:846–55
4. Tan Q, Irwin P, Cao Y. 2006. Advanced dielectrics for capacitors. *IEEJ Trans. Fundam. Mater.* 126:1152–59
5. Reaney IM, Iddles D. 2006. Microwave dielectric ceramics for resonators and filters in mobile phone networks. *J. Am. Ceram. Soc.* 89:2063–72
6. Bell AJ. 2008. Ferroelectrics: the role of ceramic science and engineering. *J. Eur. Ceram. Soc.* 28:1307–17
7. Chu BJ, Zhou X, Ren K, Neese B, Lin M, et al. 2006. A dielectric polymer with high electric energy density and fast discharge speed. *Science* 313:334–36
8. Khanchaitit P, Han K, Gadinski MR, Li Q, Wang Q. 2013. Ferroelectric polymer networks with high energy density and improved discharged efficiency for dielectric energy storage. *Nat. Commun.* 4:2845
9. Li Q, Han K, Gadinski MR, Zhang G, Wang Q. 2014. High energy and power density capacitors from solution-processed ternary ferroelectric polymer nanocomposites. *Adv. Mater.* 26:6244–49
10. Li Q, Liu F, Yang T, Gadinski MR, Zhang G, et al. 2016. Sandwich-structured polymer nanocomposites with high energy density and great charge-discharge efficiency at elevated temperatures. *PNAS* 113:9995–10000
11. Montanari D, Saarinen K, Scagliarini F, Zeidler D, Niskala M, Nender D. 2009. Film capacitors for automotive and industrial applications. In *Proc. CARTS*, Jacksonville, FL, Apr. 23–38
12. Bower D. 2000. Inverters-critical photovoltaic balance-of-system components: status, issues, and new-millennium opportunities. *Prog. Photovolt. Res. Appl.* 8:113–26

Annu. Rev. Mater. Res. 2018.48:219-243. Downloaded from www.annualreviews.org
Access provided by Copenhagen University on 05/07/22. For personal use only.

Annu. Rev. Mater. Res. 2018.48:219-243. Downloaded from www.annualreviews.org
Access provided by Copenhagen University on 05/07/22. For personal use only.

13. Tan D, Zhang L, Chen Q, Irwin P. 2014. High-temperature capacitor polymer films. *J. Electron. Mater.* 43:4569–75
14. Johnson RW, Evans JL, Jacobsen P, Thompson JR, Christopher M. 2004. The changing automotive environment: high-temperature electronics. *IEEE Trans. Electron. Packag. Manuf.* 27:164–76
15. Weimer JA. 1993. Electrical power technology for the more electric aircraft. In *Proc. AIAA/IEEE Digit. Avion. Syst. Conf., 12th*, pp. 445–50
16. Watson J, Castro G. 2012. High-temperature electronics pose design and reliability challenges. *Analog Dialogue* 46:1–7
17. Barshaw EJ, White J, Chait MJ, Cornette JB, Bustamante J, et al. 2007. High energy density (HED) biaxially-oriented poly-propylene (BOPP) capacitors for pulse power applications. *IEEE Trans. Magn.* 43:223–25
18. Rabuffi M, Picci G. 2002. Status quo and future prospects for metallized polypropylene energy storage capacitors. *IEEE. Trans. Plasma Sci.* 30:1939–42
19. Zhang S, Zou C, Kushner DI, Zhou X, Orchard RJ Jr., et al. 2012. Semicrystalline polymers with high dielectric constant, melting temperature, and charge-discharge efficiency. *IEEE Trans. Dielectr. Electr. Insul.* 19:1158–66
20. Burress TA, Coomer CL, Campbell SL, Wereszczak AA, Cunningham JP, et al. 2008. *Evaluation of the 2008 Lexus LS 600H hybrid synergy drive system*. Tech. Rep. ORNL/TM-2008/185, Oak Ridge Natl. Lab.
21. Burress TA, Coomer CL, Campbell SL, Seiber LE, Marlino LD, et al. 2007. *Evaluation of the 2007 Toyota Camry hybrid synergy drive system*. Tech. Rep. ORNL/TM-2007/190, Oak Ridge Natl. Lab.
22. Hsu J, Staunton R, Starke M. 2006. *Barriers to the application of high-temperature coolants in hybrid electric vehicles*. Tech. Rep. ORNL/TM-2006/514, Oak Ridge Natl. Lab.
23. Bennion K, Thornton M. 2010. *Integrated vehicle thermal management for advanced vehicle propulsion technologies*. Presented at SAE World Cong., Detroit, MI, SAE Tech. Pap. 2010-01-0836
24. Zhang X, Liu J, Yang S. 2016. A review on recent progress of R&D for high-temperature resistant polymer dielectrics and their applications in electrical and electronic insulation. *Rev. Adv. Mater. Sci.* 46:22–38
25. Randall CA, Ogihara H, Kim JR, Yang GY, Stringer CS, et al. 2009. *High temperature and high energy density dielectric materials*. Presented at IEEE Pulsed Power Conf., Washington, DC
26. Zhu L, Wang Q. 2012. Novel ferroelectric polymers for high energy density and low loss dielectrics. *Macromolecules* 45:2937–54
27. Wang Q, Zhu L. 2011. Polymer nanocomposites for electrical energy storage. *J. Polym. Sci. B Polym. Phys.* 49:1421–29
28. Nan CW, Shen Y, Ma J. 2010. Physical properties of composites near percolation. *Annu. Rev. Mater. Res.* 40:131–51
29. Dang ZM, Yuan JK, Yao SH, Liao RJ. 2013. Flexible nanodielectric materials with high permittivity for power energy storage. *Adv. Mater.* 25:6334–65
30. Zhu L. 2014. Exploring strategies for high dielectric constant and low loss polymer dielectrics. *J. Phys. Chem. Lett.* 5:3677–87
31. Li Q, Wang Q. 2016. Ferroelectric polymers and their energy-related applications. *Macromol. Chem. Phys.* 217:1228–44
32. Young RJ, Lovell PA. 1991. *Introduction to Polymers*. London: Chapman & Hall
33. Ieda M. 1980. Dielectric breakdown process of polymers. *IEEE Trans. Dielectr. Electr. Insul.* EI-15:206–24
34. Stark KH, Garton CG. 1955. Electric strength of irradiated polythene. *Nature* 176:1225–26
35. Zebouchi N, Bendaoud M, Essolbi R, Malec D, Ai B, Giam H. 1996. Electrical breakdown theories applied to polyethylene terephthalate films under the combined effects of pressure and temperature. *J. Appl. Phys.* 79:2497–501
36. Hanley TL, Burford RP, Fleming RJ, Barber KW. 2003. A general review of polymeric insulation for use in HVDC cables. *IEEE Electr. Insul. Mag.* 19:13–24
37. Li Q, Chen L, Gadinski MR, Zhang S, Zhang G, et al. 2015. Flexible high-temperature dielectric materials from polymer nanocomposites. *Nature* 523:576–80
38. McPherson J, Kim JY, Shanware A, Mogul H. 2003. Thermochemical description of dielectric breakdown in high dielectric constant materials. *Appl. Phys. Lett.* 82:2121

Annu. Rev. Mater. Res. 2018.48:219-243. Downloaded from www.annualreviews.org
Access provided by Copenhagen University on 05/07/22. For personal use only.

39. Chiu FC. 2014. A review on conduction mechanisms in dielectric films. *Adv. Mater. Sci. Eng.* 2014:578168
40. Ho J, Jow TR. 2012. High field conduction in biaxially oriented polypropylene at elevated temperature. *IEEE Trans. Dielectr. Electr. Insul.* 19:990–95
41. Ieda M. 1984. Electrical conduction and carrier traps in polymeric materials. *IEEE Trans. Electr. Insul.* 19:162–78
42. Ambegaokar V, Halperin BI, Langer JS. 1971. Hopping conductivity in disordered systems. *Phys. Rev. B* 4:2612
43. Neusel C, Jelitto H, Schneider GA. 2015. Electrical conduction mechanism in bulk ceramic insulators at high voltages until dielectric breakdown. *J. Appl. Phys.* 117:154902
44. Kirby AJ. 1992. *Polyimides: Materials Processing and Applications*. Oxford, UK: Pergamon Press
45. Cassidy PE, Fawcett NC. 1979. Polyimides. In *Encyclopedia of Chemical Technology*, Vol. 18, ed. HF Mark, A Standen, pp. 704–19. New York: John Wiley & Sons
46. Vanherck K, Koeckelberghs G, Vankelecom IFJ. 2013. Crosslinking polyimides for membrane applications: a review. *Prog. Polym. Sci.* 38:874–96
47. Diaham S, Zelmat S, Locatelli ML, Dinculescu S, Decup M, Lebey T. 2010. Dielectric breakdown of polyimide films: area, thickness and temperature dependence. *IEEE Trans. Electr. Insul.* 17:18–27
48. Tsukiji M, Bitoh W, Enomoto J. 1990. Thermal degradation and endurance of polyimide films. In *Electrical Insulation (Conf. Rec. 1990 IEEE Int. Symp.)*, pp. 88–91
49. Tan D, Zhang L, Chen Q, Irwin P. 2014. High-temperature capacitor polymer films. *J. Electron. Mater.* 43:4569–75
50. Venkat N, Dang TD, Bai Z, McNier VK, DeCerbo JN, et al. 2010. High temperature polymer film dielectrics for aerospace power conditioning capacitor applications. *Mater. Sci. Eng. B* 168:16–21
51. Sadana AK, Saini RK, Billups WE. 2003. Cyclobutarenes and related compounds. *Chem. Rev.* 103:1539–602
52. Schwödiauer R, Neugschwandtner GS, Bauer-Gogonea S, Bauer S, Wirges W. 1999. Low-dielectric-constant cross-linking polymers: film electrets with excellent charge stability. *Appl. Phys. Lett.* 75:3998–4000
53. Heistand R II, DeVellis R, Garrou P, Burdeaux D, Stokich T, et al. 1992. Cyclotene 3022 (BCB) for non-hermetic packaging. In *Proc. ISHM 1992*, San Francisco, Oct. 19–21, pp. 584–90
54. WIMA. *Substitution of obsolete polycarbonate (PC) capacitors*. **http://www.wimausa.com/EN/polycarbonate.htm**
55. Ho J, Jow TR. 2009. *Characterization of high temperature polymer thin films for power conditioning capacitors*. Tech. Rep. ARL-TR-4880, Army Res. Lab.
56. Cheng SZD, Ho RM, Hsiao BS, Gardner KH. 1996. Polymorphism and crystal structure identification in poly(aryl ether ketone ketone)s. *Macromol. Chem. Phys.* 197:185–213
57. Pan J, Li K, Li J, Hsu T, Wang Q. 2009. Dielectric characteristics of poly(ether ketone ketone) for high temperature capacitive energy storage. *Appl. Phys. Lett.* 95:022902
58. Pan J, Li K, Chuayprakong S, Hsu T, Wang Q. 2010. High-temperature poly(phthalazinone ether ketone) thin films for dielectric energy storage. *ACS Appl. Mater. Interface* 2:1286–89
59. Zhang X, Shen Y, Zhang Q, Gu L, Hu Y, et al. 2015. Ultrahigh energy density of polymer nanocomposites containing $BaTiO_3$@TiO_2 nanofibers by atomic-scale interface engineering. *Adv. Mater.* 27:819–24
60. Huang X, Jiang P. 2015. Core-shell structured high-k polymer nanocomposites for energy storage and dielectric applications. *Adv. Mater.* 27:546–54
61. Li Q, Zhang G, Zhang X, Jiang S, Zeng Y, Wang Q. 2015. Relaxor ferroelectric-based electrocaloric polymer nanocomposites with a broad operating temperature range and high cooling energy. *Adv. Mater.* 27:2236–41
62. Yim A, Chahal RS, St. Pierre LE. 1973. The effect of polymer-filler interaction energy on the T_g of filled polymers. *J. Colloid Interface Sci.* 43:583–90
63. Fragiadakis D, Pissis P, Bokobza L. 2005. Glass transition and molecular dynamics in poly(dimethylsiloxane)/silica nanocomposites. *Polymer* 46:6001–8
64. Tabatabaei-Yazdi Z, Mehdipour-Ataei S. 2015. Poly(ether-imide) and related sepiolite nanocomposites: investigation of physical, thermal, and mechanical properties. *Polym. Adv. Technol.* 26:308–14

65. Coleman JN, Khan U, Gun'ko YK. 2006. Mechanical reinforcement of polymers using carbon nanotubes. *Adv. Mater.* 18:689–706
66. Zhou SJ, Ma CY, Meng YY, Su HF, Zhu Z, et al. 2012. Activation of boron nitride nanotubes and their polymer composites for improving mechanical performance. *Nanotechnology* 23:055708
67. Zhi C, Bando Y, Tang C, Kuwahara H, Golberg D. 2009. Large-scale fabrication of boron nitride nanosheets and their utilization in polymeric composites with improved thermal and mechanical properties. *Adv. Mater.* 21:2889–93
68. Esfandiari A, Nazokdast H, Rashidi A-S, Yazdanshenas M-E. 2008. Review of polymer-organoclay nanocomposites. *J. Appl. Sci.* 8:545–61
69. Yu J, Mo H, Jiang P. 2015. Polymer/boron nitride nanosheet composite with high thermal conductivity and sufficient dielectric strength. *Polym. Adv. Technol.* 26:514–20
70. Fujita F, Ruike M, Baba M. 1996. Treeing breakdown voltage and TSC of alumina filled epoxy resin. *IEEE Intern. Symp. Electr. Insul.* 2:738–41
71. Wang YU, Tan DQ. 2011. Computational study of filler microstructure and effective property relations in dielectric composites. *J. Appl. Phys.* 109:104102
72. Zhang G, Zhang X, Yang T, Li Q, Chen LQ, et al. 2015. Colossal room-temperature electrocaloric effect in ferroelectric polymer nanocomposites using nanostructured barium strontium titanates. *ACS Nano* 9:7164–74
73. Tomer V, Polizos G, Randall CA, Manias E. 2011. Polyethylene nanocomposite dielectrics: implications of nanofiller orientation on high field properties and energy storage. *J. Appl. Phys.* 109:074113
74. Golberg D, Bando Y, Huang Y, Terao T, Mitome M, et al. 2010. Boron nitride nanotubes and nanosheets. *ACS Nano* 4:2979–93
75. Levy O, Stroud D. 1997. Maxwell Garnett theory for mixtures of anisotropic inclusions: application to conducting polymers. *Phys. Rev. B* 56:8035–46
76. Rao Y, Qu J, Marinis T, Wong CP. 2000. A precise numerical prediction of effective dielectric constant for polymer-ceramic composite based on effective-medium theory. *IEEE Trans. Compon. Packag. Technol.* 23:680–83
77. Wu YH, Zha JW, Yao ZQ, Sun F, Li RKY, Dang ZM. 2015. Thermally stable polyimide nanocomposite films from electrospun $BaTiO_3$ fibers for high-density energy storage capacitors. *RSC Adv.* 5:44749–55
78. Hu P, Shen Y, Guan Y, Zhang X, Lin Y, et al. 2014. Topological-structure modulated polymer nanocomposites exhibiting highly enhanced dielectric strength and energy density. *Adv. Funct. Mater.* 24:3172–78
79. Wang Y, Cui J, Yuan Q, Niu Y, Bai Y, Wang H. 2015. Significantly enhanced breakdown strength and energy density in sandwich-structured barium titanate/poly(vinylidene fluoride) nanocomposites. *Adv. Mater.* 27:6658–63
80. Wang Y, Cui J, Wang L, Yuan Q, Niu Y, et al. 2017. Compositional tailoring effect on electric field distribution for significantly enhanced breakdown strength and restrained conductive loss in sandwich-structured ceramic/polymer nanocomposites. *J. Mater. Chem. A* 5:4710–18
81. Wang Y, Wang L, Yuan Q, Niu Y, Chen J, et al. 2017. Ultrahigh electric displacement and energy density in gradient layer-structured $BaTiO_3$/PVDF nanocomposites with an interfacial barrier effect. *J. Mater. Chem. A* 5:10849–55
82. Liu F, Li Q, Cui J, Li Z, Yang G, et al. 2017. High-energy-density dielectric polymer nanocomposites with trilayered architecture. *Adv. Funct. Mater.* 27:1606292
83. Azizi A, Gadinski MR, Li Q, AlSaud MA, Wang J, et al. 2017. High-performance polymers sandwiched with chemical vapor deposited hexagonal boron nitrides as scalable high-temperature dielectric materials. *Adv. Mater.* 29:1701864
84. Yao Z, Song Z, Hao H, Yu Z, Cao M, et al. 2017. Homogeneous/inhomogeneous-structured dielectrics and their energy-storage performances. *Adv. Mater.* 29:1601727
85. Hao X. 2013. A review on the dielectric materials for high energy-storage application. *J. Adv. Dielectr.* 3:1330001
86. Lee H, Kim JR, Lanagan MJ, Trolier-McKinstry S, Randall CA, Davies PK. 2013. High-energy density dielectrics and capacitors for elevated temperatures: $Ca(Zr,Ti)O_3$. *J. Am. Ceram. Soc.* 96:1209–13
87. Shay DP, Podraza NJ, Donnelly NJ, Randall CA. 2012. High energy density, high temperature capacitors utilizing mn-doped $0.8CaTiO_3$–$0.2CaHfO_3$ ceramics. *J. Am. Ceram. Soc.* 95:1348–55

Annu. Rev. Mater. Res. 2018.48:219-243. Downloaded from www.annualreviews.org
Access provided by Copenhagen University on 05/07/22. For personal use only.

Annu. Rev. Mater. Res. 2018.48:219-243. Downloaded from www.annualreviews.org
Access provided by Copenhagen University on 05/07/22. For personal use only.

88. Randall CA, Ogihara H, Kim JR, Yang GY, Stringer CS, et al. 2009. High temperature and high energy density dielectric materials. In *Proc. 2009 IEEE Pulsed Power Conf.*, pp. 346–51
89. Ma BH, Hu ZQ, Koritala RE, Lee TH, Dorris SE, Balachandran U. 2015. PLZT film capacitors for power electronics and energy storage applications. *J. Mater. Sci. Mater. Electron.* 26:9279–87
90. Tong S, Ma BH, Narayanan M, Liu SS, Koritala R, et al. 2013. Lead lanthanum zirconate titanate ceramic thin films for energy storage. *ACS Appl. Mater. Interfaces* 5:1474–80
91. Xie ZK, Peng B, Zhang J, Zhang XH, Yue ZX, Li LT. 2015. Highly (100)-oriented $Bi(Ni_{1/2}Hf_{1/2})O_3$-$PbTiO_3$ relaxor-ferroelectric films for integrated piezoelectric energy harvesting and storage system. *J. Am. Ceram. Soc.* 98:2968–71
92. Zhao Y, Hao XH, Li ML. 2014. Dielectric properties and energy-storage performance of $(Na_{0.5}Bi_{0.5})TiO_3$ thick films. *J. Alloy. Compd.* 601:112–15
93. Xu ZS, Hao XH, An SL. 2015. Dielectric properties and energy-storage performance of $(Na_{0.5}Bi_{0.5})TiO_3$-$SrTiO_3$ thick films derived from polyvinylpyrrolidone-modified chemical solution. *J. Alloy. Compd.* 639:387–92
94. Peng BL, Zhang Q, Li X, Sun TY, Fan HQ, et al. 2015. Giant electric energy density in epitaxial lead-free thin films with coexistence of ferroelectrics and anti-ferroelectrics. *Adv. Electron. Mater.* 1:1500052
95. Pan H, Zeng Y, Shen Y, Lin YH, Ma J, et al. 2017. $BiFeO_3$-$SrTiO_3$ thin film as new lead-free relaxor-ferroelectric capacitor with ultrahigh energy storage performance. *J. Mater. Chem. A* 5:5920–26
96. Dittmer R, Jo W, Damjanovic D, Roödel J. 2011. Lead-free high-temperature dielectrics with wide operational range. *J. Appl. Phys.* 109:034107
97. Li F, Zhai J, Shen B, Liu X, Yang K, et al. 2017. Influence of structural evolution on energy storage properties in $Bi_{0.5}Na_{0.5}TiO_3$-$SrTiO_3$-$NaNbO_3$ lead-free ferroelectric ceramics. *J. Appl. Phys.* 121:054103
98. Ogihara H, Randall CA, Trolier-McKinstry S. 2009. Weakly coupled relaxor behavior of $BaTiO_3$-$BiScO_3$ ceramics. *J. Am. Ceram. Soc.* 92:110–18
99. Ogihara H, Randall CA, Trolier-McKinstry S. 2009. High-energy density capacitors utilizing $0.7BaTiO_3$–$0.3BiScO_3$ ceramics. *J. Am. Ceram. Soc.* 92:1719–24
100. Michael EK, Trolier-McKinstry S. 2015. Bismuth pyrochlore thin films for dielectric energy storage. *J. Appl. Phys.* 118:054101
101. Michael EK, Trolier-McKinstry S, Brennecka G. 2015. Cubic pyrochlore bismuth zinc niobate thin films for high-temperature dielectric energy storage. *J. Am. Ceram. Soc.* 98:1223–29
102. Kwon DK, Lee MH. 2012. Temperature-stable high-energy-density capacitors using complex perovskite thin films. *IEEE Trans. Ultrason. Ferroelectr. Freq. Control* 59:1894–99
103. Correia TM, McMillen M, Rokosz MK, Weaver PM, Gregg JM, et al. 2013. A lead-free and high-energy density ceramic for energy storage applications. *J. Am. Ceram. Soc.* 96:2699–702
104. Tinberg DS, Trolier-McKinstry S. 2007. Structural and electrical characterization of $x BiScO_3$–$(1-x)BaTiO_3$ thin films. *J. Appl. Phys.* 101:024112
105. Hao XH, Zhai JW, Yao X. 2009. Improved energy storage performance and fatigue endurance of Sr-doped $PbZrO_3$ anti-ferroelectric thin films. *J. Am. Ceram. Soc.* 92:1133–35
106. Zhao Y, Hao XH, Zhang Q. 2014. Energy-storage properties and electrocaloric effect of $Pb_{(1-3x/2)}La_xZr_{0.85}Ti_{0.15}O_3$ anti-ferroelectric thick films. *ACS Appl. Mater. Interfaces* 6:11633–39
107. Ge J, Remiens D, Dong X, Chen Y, Costecalde J, et al. 2014. Enhancement of energy storage in epitaxial $PbZrO_3$ anti-ferroelectric films using strain engineering. *Appl. Phys. Lett.* 105:112908
108. Liu C, Lin SX, Qin MH, Lu XB, Gao XS, et al. 2016. Energy storage and polarization switching kinetics of (001)-oriented $Pb_{0.97}La_{0.02}(Zr_{0.95}Ti_{0.05})O_3$ anti-ferroelectric thick films. *Appl. Phys. Lett.* 108:112903
109. Park MH, Kim HJ, Kim YJ, Moon T, Kim KD, Hwang CS. 2014. Thin $Hf_xZr_{1-x}O_2$ films: a new lead-free system for electrostatic supercapacitors with large energy storage density and robust thermal stability. *Adv. Energy Mater.* 4:1400610
110. Shimizu H, Guo H, Reyes-Lillo SE, Mizuno Y, Rabe KM, Randall CA. 2015. Lead-free anti-ferroelectric: $x CaZrO_3$-$(1-x)NaNbO_3$ system ($0 \le x \le 0.10$). *Dalton Trans.* 44:10763–72
111. Guo H, Shimizu H, Mizuno Y, Randall CA. 2015. Strategy for stabilization of the anti-ferroelectric phase (*Pbma*) over the metastable ferroelectric phase ($P2_1ma$) to establish double loop hysteresis in lead-free $(1-x)NaNbO_3$-$xSrZrO_3$ solid solution. *J. Appl. Phys.* 117:214103

112. Kobayashi K, Ryu M, Doshida Y, Mizuno Y, Randall CA, Tan X. 2012. Novel high-temperature antiferroelectric-based dielectric $NaNbO_3$-$NaTaO_3$ solid solutions processed in low oxygen partial pressures. *J. Am. Ceram. Soc.* 96:531–37
113. Zhao L, Liu Q, Zhang SJ, Li J-F. 2016. Lead-free $AgNbO_3$ anti-ferroelectric ceramics with enhanced energy storage performance by MnO_2 modification. *J. Mater. Chem. C* 4:8380–84
114. Zhao L, Liu Q, Gao J, Zhang SJ, Li J-F. 2017. Lead-free anti-ferroelectric silver niobate tantalate with high energy storage performance. *Adv. Mater.* 29:1701824
115. Xu R, Tian JJ, Zhu QS, Zhao T, Feng YJ, et al. 2017. Effects of phase transition on discharge properties of PLZST anti-ferroelectric ceramics. *J. Am. Ceram. Soc.* 100:3618–25
116. Xu R, Xu Z, Feng Y, Wei X, Tian J. 2016. Nonlinear dielectric and discharge properties of $Pb_{0.94}La_{0.04}[(Zr_{0.56}Sn_{0.44})_{0.84}Ti_{0.16}]O_3$ anti-ferroelectric ceramics. *J. Appl. Phys.* 120:144102
117. Liu Z, Chen XF, Peng W, Xu CH, Dong XL, et al. 2015. Temperature-dependent stability of energy storage properties of $Pb_{0.97}La_{0.02}(Zr_{0.58}Sn_{0.335}Ti_{0.085})O_3$ anti-ferroelectric ceramics for pulse power capacitors. *Appl. Phys. Lett.* 106:262901
118. Zhang L, Jiang SL, Fan BY, Zhang GZ. 2015. High energy storage performance in $(Pb_{0.858}Ba_{0.1}Ln_{0.02}Y_{0.008})(Zr_{0.65}Sn_{0.3}Ti_{0.05})O_3(Pb_{0.97}La_{0.02})(Zr_{0.9}Sn_{0.05}Ti_{0.05})O_3$ anti-ferroelectric composite ceramics. *Ceram. Int.* 41:1139–44
119. Yi J, Zhang L, Xie B, Jiang S. 2015. The influence of temperature induced phase transition on the energy storage density of anti-ferroelectric ceramics. *J. Appl. Phys.* 118:124107
120. Hu G, Ma C, Wei W, Sun Z, Lu L, et al. 2016. Enhanced energy density with a wide thermal stability in epitaxial $Pb_{0.92}La_{0.08}Zr_{0.52}Ti_{0.48}O_3$ thin films. *Appl. Phys. Lett.* 109:193904
121. Liu Y, Hao X, An S. 2013. Significant enhancement of energy-storage performance of $(Pb_{0.91}La_{0.09})(Zr_{0.65}Ti_{0.35})O_3$ relaxor ferroelectric thin films by Mn doping. *J. Appl. Phys.* 114:174102
122. Zhang L, Hao X, Yang J, An S, Song B. 2013. Large enhancement of energy-storage properties of compositional graded $(Pb_{1-x}La_x)(Zr_{0.65}Ti_{0.35})O_3$ relaxor ferroelectric thick films. *Appl. Phys. Lett.* 103:113902
123. Zhao Y, Hao XH, Zhang Q. 2016. Enhanced energy-storage performance and electrocaloric effect in compositionally graded $Pb_{(1-3x/2)}La_xZr_{0.85}Ti_{0.15}O_3$ anti-ferroelectric thick films. *Ceram. Int.* 42:1679–87
124. Sun ZX, Ma CR, Liu M, Cui J, Lu L, et al. 2016. Ultrahigh energy storage performance of lead-free oxide multilayer film capacitors via interface engineering. *Adv. Mater.* 29:1604427
125. Ortega N, Kumar A, Scott JF, Douglas BC, Tomazawa M, et al. 2012. Relaxor-ferroelectric superlattices: high energy density capacitors. *J. Phys. Condens. Matter* 24:445901
126. Correia T, Stewart M, Ellmore A, Albertsen K. 2017. Lead-free ceramics with high energy density and reduced losses for high temperature applications. *Adv. Eng. Mater.* 19:1700019
127. Wang CC, Pilania G, Boggs SA, Kumar S, Breneman C, Ramprasad R. 2014. Computational strategies for polymer dielectrics design. *Polymer* 55:979–88
128. Han K, Li Q, Chanthad C, Gadinski MR, Zhang G, Wang Q. 2015. A hybrid material approach toward solution-processable dielectrics exhibiting enhanced breakdown strength and high energy density. *Adv. Funct. Mater.* 25:3505–13
129. Kim GH, Lee D, Shanker A, Shao L, Kwon MS, et al. 2015. High thermal conductivity in amorphous polymer blends by engineered interchain interactions. *Nat. Mater.* 14:295–300

Annu. Rev. Mater. Res. 2018.48:219-243. Downloaded from www.annualreviews.org
Access provided by Copenhagen University on 05/07/22. For personal use only.

Annual Review of Materials Research

Volume 48, 2018

Contents

Annu. Rev. Mater. Res. 2018.48:219-243. Downloaded from www.annualreviews.org
Access provided by Copenhagen University on 05/07/22. For personal use only.

Indexes

Errata

An online log of corrections to *Annual Review of Materials Research* articles may be found at http://www.annualreviews.org/errata/matsci

Annu. Rev. Mater. Res. 2018.48:219-243. Downloaded from www.annualreviews.org
Access provided by Copenhagen University on 05/07/22. For personal use only.